The Gut Microbiome Was Associated With Brain Structure and Function in Schizophrenia

Shijia Li
South China University of Technology
Jie Song
South China University of Technology
Pengfei Ke
South China University of Technology
Lingyin Kong
South China University of Technology
Bingye Lei
South China University of Technology
Jing Zhou
South China University of Technology
Yuanyuan Huang
The Affiliated Brain Hospital of Guangzhou Medical University, Guangzhou Huiai Hospital
Hehua Li
The Affiliated Brain Hospital of Guangzhou Medical University, Guangzhou Huiai Hospital
Guixiang Li
Guangdong Engineering Technology Research Center for Diagnosis and Rehabilitation of Dementia
Jun Chen
Guangdong Engineering Technology Research Center for Diagnosis and Rehabilitation of Dementia
Xiaobo Li
Guangdong Engineering Technology Research Center for Translational Medicine of Mental Disorders
Zhiming Xiang
Guangdong Engineering Technology Research Center for Diagnosis and Rehabilitation of Dementia
Yuping Ning
The Affiliated Brain Hospital of Guangzhou Medical University, Guangzhou Huiai Hospital
Fengchun Wu
The Affiliated Brain Hospital of Guangzhou Medical University, Guangzhou Huiai Hospital
Kai Wu (kaiwu@scut.edu.cn)
South China University of Technology

Research Article

Keywords: schizophrenia (SZ), gut microbiome, brain structure and function, microbiome-gut-brain (MGB) axis

Posted Date: February 11th, 2021

DOI: https://doi.org/10.21203/rs.3.rs-181659/v1

Abstract

The effects of the gut microbiome on the central nervous system and its possible role in mental disorders have received increasing attention. However, our knowledge about the relationship between the gut microbiome and brain structure and function is still very limited. Here, we leveraged 16S rRNA sequencing with structural magnetic resonance imaging (sMRI) and resting-state functional (rs-fMRI) to investigate differences in fecal microbiota between 38 patients with schizophrenia (SZs) and 38 demographically matched normal controls (NCs) and explored whether such differences were associated with brain structure and function. At the genus level, we found that the relative abundance of *Ruminococcus* and *Roseburia* was significantly lower, whereas the abundance of *Veillonella* was increased in SZs compared to NCs. Additionally, the MRI results revealed that several brain regions showed lower gray matter volume (GMV) and regional homogeneity (ReHo), but increased amplitude of low-frequency fluctuation (ALFF) in SZs than in NCs. Statistical analyses were performed to explore the associations between microbial shifts and brain structure and function. Alpha diversity of gut microbiota showed a strong linear relationship with GMV and ReHo. Moreover, we found that lower ReHo indexes in the right STC (r = -0.35, p = 0.031, FDR corrected p = 0.039), the left cuneus (r = -0.33, p = 0.044, FDR corrected p = 0.053) and the right MTC (r = -0.34, p = 0.03, FDR corrected p = 0.052) were negatively correlated with a lower abundance of the genus *Roseburia*. This study suggests that the potential role of the gut microbiome in schizophrenia (SZ) is related to the alteration of brain structure and function, suggesting a new direction for studying the pathology of SZ.

Introduction

With the advent of sequencing technology, characterization of schizophrenia (SZ) with probing of the underlying gut microbiome can provide abundant clues for the diagnosis and prognosis of SZ [1]. Several published studies of the gut microbiome in SZ revealed that the species composition within the gut of individuals with SZ is different from that of normal control subjects (NCs), with varying bacterial taxa driving community separation in each study, and several of these studies have also focused on the relationship between different gut microbiota and clinical characteristics [2-4]. Converging evidence suggests that the gut microbiota communicates with the central nervous system bidirectionally through the microbiome-gut-brain (MGB) axis [5,6]. A dysregulated MGB axis has been reported in many neuropsychiatric disorders, including SZ [7], depression [8], bipolar disorder [9], autism [10], Alzheimer's disease [11], and Parkinson's disease [12]. Gut microbiota can control the expression of a variety of neurotrophic factors, such as brain-derived neurotropic factor (BDNF) and glial cell line-derived neurotrophic factor (GDNF), which can affect neural development and plasticity in the brain [13]. New findings regarding the MGB axis in SZ have recently been reported. Nguyen et al. [14] suggested that SZ is associated with gastrointestinal inflammation. Additionally, gut and digestive disturbances are highly prevalent comorbidities in SZs [15]. However, few studies have reported on the relationship between the gut microbiome and brain structure and function.

Magnetic resonance imaging (MRI) techniques have been widely adopted to study abnormalities in brain structure and function in SZs [16]. Meta-analysis found that SZs showed widespread attenuation of cortical thickness and surface area especially in frontal and temporal regions compared with NCs [17] . Voxel-based morphometry (VBM) analysis found that SZ patients showed reduced gray matter volume (GMV) in insular subregions [18]. The alteration of brain function was also observed in SZ patients [19]. As one of the methods to measure local resting functional connectivity (FC) or synchronization [20], regional homogeneity (ReHo) represents the most efficient, reliable, and widely used index beyond the different FC metrics [21,22]. The calculation of ReHo assumes that a given voxel is

temporally similar to that of its neighbors [23]. Specifically, taking the voxel or vertex of high-resolution connectomes in the graph as a node, the ReHo index of this node is computed as Kendall's coefficient of concordance (KCC) [23]. Previous studies found that SZs often showed increased ReHo in the inferior and middle temporal area [22], the bilateral superior medial prefrontal cortex (mPFC) [20], the right superior frontal gyrus, the right superior temporal cortex (STC) [24] and the fusiform gyrus [22] but decreased ReHo in the right precentral lobule, the right inferior parietal lobule (IPL), the left paracentral lobule [20], the left postcentral gyrus and the left STG [24] compared with those of NCs. Additionally, amplitude of low-frequency fluctuation (ALFF) has been widely used as a neuroimage biomarker to explore the resting-state regional brain activity in psychiatric disorders, including schizophrenia [25]. A meta-analysis of resting-state functional MRI (rs-fMRI) reported decreased ALFF in the bilateral postcentral gyrus, bilateral precuneus, left inferior parietal gyri and right occipital lobe, and increased ALFF in the right putamen, right inferior frontal gyrus, left inferior temporal gyrus and right anterior cingulate cortex in SZs [26].

In the present study, we hypothesized that in SZs, the differences in gut microbial composition might be related to the differences in the GMV, ReHo and ALFF indexes between SZs and NCs. To this end, we recruited 76 participants, including 38 SZs and 38 NCs, and then collected their rs-fMRI data and stool samples. Next, 16S rRNA sequencing was applied to analyze the composition of the gut microbiome, GMV index was calculated to explore brain structure alteration, and ReHo and ALFF indexes were calculated to explore functional brain activity. Finally, we calculated the correlation between the gut microbiome and the GMV, ReHo and ALFF indexes, which showed differences between the two groups.

Methods

Participants

A total of 76 subjects were recruited, including 38 SZs recruited from the Affiliated Brain Hospital of Guangzhou Medical University and 38 age-, sex- and BMI-matched NCs recruited in Guangzhou and surrounding areas. The diagnosis of SZ was made based on the Diagnostic and Statistical Manual of Mental Disorder-IV-Text Revision (DSM-IV-TR) (SCID). Patients with stable psychiatric symptoms for > 2 weeks and a total Positive and Negative Syndrome Scale (PANSS) score of $\geq$ 30 with a rate of change of $\leq$ 20% in 2 weeks were included in the study. Thirty-five of the patients were on antipsychotic medication at the time of the study. The exclusion criteria for all participants included 1) any other current major DSM-IV-TR Axis I diagnoses; 2) any somatic diseases; 3) a history of epilepsy, except for febrile convulsions; 4) a history of having received electroconvulsive therapy in the past 6 months; 5) lactating, pregnant, or planning to become pregnant; 6) alcohol dependence or 7) noncompliance with drug administration or a lack of legal guardians.

The study protocol was approved by the ethics committees of the Affiliated Brain Hospital of Guangzhou Medical University, and written informed consent was obtained from each subject or their legal guardian prior to the study. A questionnaire was conducted among all subjects to collect general information, including age, sex, BMI, years of education, history of medication used and history of smoking and drinking.

Fecal sample collection and processing

Fresh fecal samples were collected from participants after fasting for 12 hours, and all of the samples were stored at -80°C until DNA extraction. A total of 200 mg of each fecal sample was used for DNA extraction. The method of

DNA extraction was similar to the protocol described in our previous work [4].

MRI data collecting and preprocessing

MRI data were acquired on a Philips Achieva 3T MRI Scanner in the Affiliated Brain Hospital of Guangzhou Medical University. The functional data were obtained using an echo-planar imaging (EPI) sequence with the following parameters: repetition time (TR) = 9,000 ms, echo time (TE) = 30 ms, flip angle = 90°, field of view (FOV) = 211 mm ×211 mm, data matrix = 64 × 64, voxel size = 3.44 × 3.44 × 4.6 mm^3. High-resolution brain structural images were obtained using a T1-weighted 3D gradient-echo sequence (TR = 8.2 ms, TE = 3.8 ms, flip angle = 7°, data matrix = 256 × 256, voxel size = 1 × 1 × 1 mm^3). Each study participant was instructed to keep their eyes closed, to relax but not fall asleep, and to move as little as possible.

The structural data were preprocessed using SPM 12 (https://www.fil.ion.ucl.ac.uk/spm/) and DPABI (version 4.3, http://rfmri.org/dpabi). The GMV was calculated as follows: we first segmented the original T1-weighted images into gray matter (GM), white matter (WM), and cerebrospinal fluid (CSF) images. Then the segmented GM images for all the subjects were used to create a customized Diffeomorphic Anatomical Registration using Exponentiated Lie algebra (DARTEL) [60] template. Afterwards, the GM images were warped to the DARTEL-template and spatially normalized to the Montreal Neurological Institute (MNI) space with modulation. Next, the modulated images were smoothed with a Gaussian kernel of 8 mm FWHM [61]. Finally, we extracted the value of GMV of each brain region segmented by the Anatomical Automatic Labeling (AAL) atlas for each subject from the modulated and smoothed images.

The functional data were preprocessed using SPM 12 (https://www.fil.ion.ucl.ac.uk/spm/) and DPABI (version 4.3, http://rfmri.org/dpabi). For each subject, we performed the preprocessing as follows: First, we removed the first 10 time points to eliminate the nonuniform magnetic field and patient inadaptability to the environment, then we performed slice timing correction, and the images were realigned to the first volume for head motion correction. Subsequently, we co-registered the functional images to the individual structural images and then normalized them in Montreal neurological institute (MNI) standard space by using an affine transformation with the voxels being resampled to 3 × 3 × 3 mm^3 isotropic voxels. Finally, the resampled data were bandpass (0.01–0.08 Hz) filtered to reduce low-frequency drift and high-frequency physiological noise and spatially smoothed with a Gaussian kernel of 4 mm full width at half maximum (FWHM). After that, we extracted the ReHo and ALFF indexes of each subject from the preprocessed images.

The ReHo index was calculated as follows: first, the ReHo index of each voxel was denoted by Kendall's coefficient of concordance (KCC) of the time series of this voxel with its 26 nearest neighbors [45]. Then, the raw ReHo index of each voxel was divided by the global mean ReHo index for each subject to reduce the global effects of variability across the participants [62]. Subsequently, the individual ReHo maps were partitioned into 1,024 ROIs, and the mean ReHo index of each region was acquired by averaging the ReHo indexes within that region. Finally, we obtained the ReHo index of each brain region segmented by the AAL atlas for each subject.

The ALFF index was calculated as follows: first, each voxel of the time series was converted to the frequency domain by using fast Fourier transformation [28]. Then, the square root of the power spectrum was calculated and was averaged across a predefined frequency range. ALFF is the averaged square root, which reflected the absolute

intensity of spontaneous brain activity. Finally, the whole brain voxel average ALFF was divided to reduce the global effects of variability across subjects to achieve standardization [63].

Statistical analyses of bioinformatics and brain function

Sequencing of the V4 region of the 16S rRNA gene was performed on the Illumina MiSeq platform. Sequence data were processed to concatenate reads into tags according to the overlapping relationship by using QIIME2 [64]. The raw sequencing results were demultiplexed and quality controlled by applying the DADA2 [65] algorithm to generate feature sequences. The output features were rarefied to 13,500 sequences per sample, which was the lowest value in the dataset. Features containing fewer than 2 sequences or those present in less than 20% of the subjects were filtered out. Microbial community structure was characterized using measures of alpha diversity and beta diversity. The alpha diversity indexes we selected were evenness, Faith's phylogenetic diversity (Faith_PD), observed species and the Shannon index. Since the sequence number of fecal sample from one SZ subject was lower than the set sampling depth (13500), this sample was dropped from the alpha diversity analysis. The differences in diversity between groups were calculated using the nonparametric Kruskal-Wallis *H* test in QIIME2. The Bray-Curtis dissimilarity of beta diversity indicates differences in taxa composition between samples based on quantitative species abundance data, which may be presented in a distance matrix. Output matrices were ordinated and visualized using the vegan package from R [66]. A classifier for taxonomy analysis was trained based on sequences and taxonomic results from the Greengenes database (http://greengenes.lbl.gov).

The taxonomic table was normalized to the relative abundances at different taxa levels, and 1321 features and 153 genera were obtained. All differential abundances at the genus level were tested using the Mann-Whitney *U* test. Two-sample *t*-tests were performed on the MRI indexes to compare the differences in functional brain activity between the SZs and NCs. To determine the association between differential abundance at the genus level and the MRI indexes, we further calculated the residuals of the relative abundances of those taxa and MRI indexes with significant group differences, controlling for age, gender and years of education, by the 'vglm' function in the VGAM package [67]. Pearson's correlations were then calculated between the residuals of the relative abundances of the altered genera and the different MRI indexes. The significances of all tests were set at $p < 0.05$ or FDR corrected $p < 0.05$ (two-sided).

Results

Clinical data

The cohort investigated in this study comprised 38 SZs and 38 NCs who did not differ in terms of age, sex, BMI or several other parameters ($p > 0.05$). SZs had higher rates of smoking ($p = 0.03$), longer sleep times ($p = 0.007$) and fewer years of education ($p = 0.01$). However, in terms of alcohol intake, there was a higher rate of alcohol consumption in the NC group ($p < 0.001$) (Table 1).

Table 1. Demographic characteristics of the NC and SZ subjects

Characteristic	NC (n = 38)	SZ (n = 38)	*p* value
Age (years)	35.47 ± 11.54	35.26 ± 10.76	0.94
Gender (M/F)	22/16	20/18	0.82
BMI (kg/m^2)	22.63 ± 2.63	23.70 ± 4.54	0.28
Education (years)	14.42 ± 2.93	12.26 ± 4.11	0.01
Sleep time (hours)	7.31 ± 0.73	8.43 ± 1.98	0.007
Alcohol	47.37%	0%	< 0.001
Smoker	2.63%	21.05%	0.03
Diastolic pressure (mmHg)	77.84 ± 8.18	77.26 ± 9.61	0.82
Systolic pressure (mmHg)	118.45 ± 9.93	115.91 ± 17.08	0.54
PANSS positive score	-	10.81 ± 5.50	-
PANSS negative score	-	17.89 ± 8.28	-
PANSS general score	-	27.71 ± 8.23	-
PANSS total score	-	56.95 ± 19.51	-
HDLC (mmol/L)	1.60 ± 0.30	1.54 ± 0.35	0.39
LDLC (mmol/L)	3.37 ± 0.85	3.20 ± 0.83	0.38
Glu (mmol/L)	5.80 ± 1.42	5.23 ± 1.25	0.07

Notes: BMI, body mass index; HDLC, high-density lipoprotein cholesterol; LDLC, low-density lipoprotein cholesterol; Glu, glucose.

Sequencing data and bacterial taxonomic composition

There was no difference between the two groups in any assessed measure of alpha diversity (Supplementary Table S1). To determine whether the overall gut microbiome composition differed between the two groups, we performed principal coordinate analysis (PCoA) of Bray-Curtis distance. As shown in Fig.1, we found significant group difference in Bray-Curtis distance (pseudo-F = 1.71, $p = 0.019$) under 999 times permutation, and PCoA of Bray-Curtis distance showed that the SZ and NC groups formed distinct clusters.

The bacterial composition results showed that sequences from NCs were mainly assigned to *Faecalibacterium*, *Megamonas*, *Roseburia* and *Gemmiger* at the genus level; the most abundant genus in SZs was also *Faecalibacterium*, followed by *Megamonas*, *Ruminococcus* and *Akkermansia* (Fig. 2a). Compared to those in the NC group, the relative abundances of *Ruminococcus* ($p = 0.017$, uncorrected), *Roseburia* ($p = 0.023$, uncorrected) and *Veillonella* ($p = 0.047$, uncorrected) were significantly lower in the SZ group (Fig. 2b).

Differences in MRI indexes between the SZs and NCs

We found that for the GMV, totally 16 brain regions segmented by AAL atlas showed significantly different between SZs and NCs, for the ReHo, totally 34 brain regions in SZs were distinct from the NCs, and totally 1 brain region's ALFF index were altered in SZs. See The detailed information in Supplementary Table S2 in the Supplementary Materials.

Relationship with MRI indexes

Figure 3 shows the significant relationship between the diversity of the microbiome and MRI indexes. Both the alpha diversity Faith_PD and observed species were correlated with GMV of the bilateral insula and right postcentral gyrus ($p < 0.05$). Meanwhile, Faith_PD showed positive correlation with the GMV of the left inferior operculum frontal cortex ($p < 0.05$). Both evenness and Shannon indexes in SZs were positively associated with the ReHo indexes of the bilateral calcarine cortex, bilateral lingual gyrus, left superior occipital cortex and right superior parietal cortex ($p < 0.05$). Additionally, evenness of alpha diversity showed positive correlations with the ReHo indexes of the right cuneus lobe, bilateral fusiform gyrus, left postcentral gyrus and left superior parietal cortex ($p < 0.05$). No significant correlation was detected between the microbial diversity and the ALFF index. The detailed information of the correlation between the microbial diversity and MRI indexes is listed in Supplementary Table S3.

After identifying both genera and MRI indexes showing significant group difference, we further tested for associations between the abundance of each genera and MRI indexes. For the brain regions segmented by the AAL atlas, we found that lower ReHo indexes in the right STC ($r = -0.35$, $p = 0.031$, FDR = 0.039), left cuneus ($r = -0.33$, $p = 0.044$, FDR = 0.053) and right MTC ($r = -0.34$, $p = 0.03$, FDR = 0.052) were negatively correlated with a lower abundance of the genus *Roseburia*. The relationships between the relative abundance of *Roseburia* and the ReHo indexes of 3 brain regions are shown in Fig. 4.

Discussion

To the best of our knowledge, this is the first study to indicate a correlation between the gut microbiome and brain structure and function in SZs. The main findings are as follows: 1) Consistent with previous studies, significant between-group differences in gut microbiota and MRI indexes were found; 2) Both the alpha diversity evenness and Shannon indexes showed a positive correlation with the GMV and ReHo indexes in several brain regions; and 3) A lower ReHo indexes in the right STC, left cuneus and right MTC were negatively correlated with a lower relative abundance of the genus *Roseburia*.

The results from 16S rRNA sequencing demonstrated significant changes in microbial composition from the Bray-Curtis distances between the two groups, suggesting greater intragroup differences in the gut microbiome of SZs. Furthermore, shifts in taxonomic abundance in SZs were consistent with previous studies. For instance, *Roseburia* (order *Clostridiales*) and *Ruminococcus* (order *Lactobacillales*) showed depletion in SZs, which was observed in multiple previous studies on psychiatric diseases [4,27,28]. *Roseburia* and *Ruminococcus* are representative bacteria that produce short-chain fatty acids (SCFAs) [29]. Microbial-derived SCFAs can cross the blood-brain barrier (BBB) and activate specific receptors in relevant brain regions pertinent to depression and anxiety-related behaviors [30]. In fact, the decrease in the relative abundance of *Roseburia* may be detrimental to insulin sensitivity and thus affect the concentrations of branched-chain amino acids (BCAAs) [31]. Due to the brain transporters shared between BCAAs and tryptophan, the presence of excessive BCAAs would cause decreased efficiency in the transportation of

tryptophan. It has been reported that excessive consumption of BCAAs could lead to decreased cerebral concentrations of tryptophan, the precursor of serotonin, and thus result in decreased cerebral 5-hydroxytryptamine concentrations [32]. Li et al. [33] speculated that depletion of the *Clostridiales* taxa, which degrade BCAAs, leads to an elevated concentration of BCAAs in the circulatory system and therefore indirectly decreases cerebral serotonin concentrations that regulate mood.

In this study we found the presence of structural abnormalities in SZs. Our results showed that the GMV of some brain regions, including the bilateral insula, frontal and temporal (see Supplementary Table S2 for the detailed regions) in SZs were decreased compared with NCs. These results are in line with previous studies which found that SZs showed decreased GMV in the insula [34], superior temporal pole [35], amygdala, anterior cingulate, and frontal cortices (superior, middle, opercular inferior, and orbital frontal gyrus) [34,35]. Van Rheenen et al. reported the entire cortex volume reductions in SZs with cognitive impairments [36]. Actually, a larger cortical volume or greater grey matter density in most brain regions is often associated with better computational efficacy [37]. Thus, we inferred that the cognitive impairments may related with the reduction of GMV in SZs.

We found that most brain regions showed a lower functional brain activity in SZs than those in NCs (Supplementary Table S2). This result is consistent with previous studies that reported altered ReHo in SZs in the bilateral STC [38], the MTC [22,38], the bilateral superior medial prefrontal cortex (mPFC) [20], the right superior frontal gyrus (SFG), and the fusiform gyrus [20,22] compared with those in NCs. Most of the brain regions that showed altered ReHo, such as the STG, MTC and SFG, are related to visual and auditory perception and are mainly located in the frontal and temporal areas (Supplementary Table S2). Several studies have reported that temporal lobe abnormalities may be related to the emergence of auditory hallucinations [39], abnormal language processing [39], thought disorder [40], and other psychotic symptoms in SZs. Additionally, the frontal lobe mediates a number of important processes that may impact executive function, working memory, abstract reasoning, social behavior, empathy, self-monitoring, and impulse control in SZ [39,41]. We also found that SZs showed increased ALFF in the right caudate than NCs (Supplementary Table S2). Previous studies reported that SZs showed significantly increased ALFF in the right caudate nucleus [42,43], middle temporal gyrus, inferior parietal lobule [42], bilateral prefrontal and parietal cortex, and left superior temporal cortex [43] compare with NCs. These findings suggested that the local synchronization of spontaneous activity and amplitude of fluctuation in SZ brains was widely disrupted, which could explain the psychopathology of SZ.

We observed significant positive associations between the gut microbial diversity measures and the reduction GMV in SZs (Fig. 3). Previous studies found that variations of genes were associated with GMV reduction in SZs, especially in the prefrontal cortex and anterior cingulate cortex [44-46]. The transcription-neuroimaging association analysis found that expression levels of 98 genes were significantly correlated with GMV changes in SZs [47]. Although no prior study reported the relationship between GMV and gut microbiome in SZs, decreased structural integrity of both white and gray matter regions including hippocampus in mice that were colonized with attention-deficit/hyperactivity disorder (ADHD) microbiota [48]. A study reported that the relative abundance of *Bacteroides* showed greater prominence in the cerebellum, frontal regions, and the hippocampus in women, which further explained that microbial modulation may affect mood and behavior [49].

Some microbiota have been reported to be associated with brain function. *Prevotella* has been shown to be associated with the development of brain abscesses and other neurological syndromes via production of IgA

proteases that promote virulence and initiate an immune response [50,51]. Lin et al. reported that the genus *Neisseria* is negatively associated with functional network connectivity (FNC) loading, especially the FNC between the left angular gyrus and right inferior occipital gyrus, which is related to visual processing function [52]. In addition, members of the genus *Neisseria*, including the species *Neisseria meningitidis*, stimulate the immune system through a variety of mechanisms and invade the neurological nervous system during infection [53]. In this study, we found that the depletion of the genus *Roseburia* was significantly associated with the local synchronization of spontaneous activity of the right STC and the right MTC, which are related to auditory verbal hallucinations [54,55] and thought disturbances [56] in SZs. Dhiman et al. [57] reported that *Roseburia* was associated with good cognitive performance, which may further support our findings. A preliminary study on the gut microbiome and brain functional connectivity in infants revealed that alpha diversity was significantly associated with functional connectivity between the amygdala and thalamus, and between the anterior cingulate cortex and anterior insula [58], suggesting a potential pathway linking gut microbial diversity and cognitive outcomes. We found that both evenness and Shannon of microbial diversity in SZs were positively associated with ReHo indexes of the bilateral calcarine cortex, bilateral lingual gyrus, left superior occipital cortex and right superior parietal cortex. Additionally, evenness showed positive correlations with ReHo indexes of the right cuneus lobe, bilateral fusiform gyrus, left postcentral gyrus and left superior parietal cortex (Table S3). We inferred that the sensory and cognitive impairments may be related to the alteration of ReHo indexes and microbial alpha diversity in SZs. For example, gut microbial alpha diversity in SZs may be associated with visual hallucinations [54,59], and this relationship could be mediated by functional brain activity in the calcarine cortex.

The present study has several limitations. First, the SZs varied considerably in their medications. Specifically, the durations and types of medication for the SZs were distinct. It is important to note that medication can affect microbiota composition and brain activity, which may further affect the results. Second, although we detected correlations between the MRI indexes and microbiota composition as well as diversity, we cannot determine the causal relationship between them. A future longitudinal study may contribute to solving this problem. Finally, the sample size was moderate. A larger independent sample is needed to examine the reproducibility of our findings.

Conclusion

In summary, the current study detected a correlation between the gut microbiome and functional brain activity in SZs. We found that both Faith_PD and observed species of alpha diversity were correlated with GMV of the bilateral insula and right postcentral gyrus. Meanwhile, the Faith_PD showed positive correlation with GMV of the left inferior operculum frontal cortex. Both evenness and Shannon indexes of alpha diversity in SZs were positively associated with ReHo indexes of the bilateral calcarine cortex, bilateral lingual gyrus, left superior occipital cortex and right superior parietal cortex. Meanwhile, the evenness showed positive correlations with ReHo indexes of the right cuneus lobe, bilateral fusiform gyrus, left postcentral gyrus and left superior parietal cortex. Additionally, we found that lower ReHo indexes in the right STC, left cuneus and right MTC were negatively correlated with a lower abundance of the genus *Roseburia*. These findings indicated that the property of the gut microbiome may be associated with the alteration of brain structure and functional brain activity in SZs.

Declarations

Declaration of Interest

The authors declare that they have no competing financial interests.

Author contributions

S.L.: Formal analysis; Investigation; Methodology; Software; Visualization; Writing - original draft; Writing - review & editing; **J.S.**: Formal analysis; Investigation; Methodology; Software; Visualization; Writing - original draft; Writing - review & editing; **P.K**: Formal analysis; Writing - review & editing; **L.K.**: Formal analysis; Writing - review & editing; **B.L.**: Formal analysis; Writing - review & editing; **J.Z.**: Writing - review & editing; **Y.H.**: Data curation; **H.L.**: Data curation; **G.L.**: Data curation; **J.C.**: Data curation; **X.L.**: Writing - review & editing; **Z.X.**: Data curation; **Y.N.**: Data curation; **F.W.**: Data curation; Funding acquisition; Project administration; Resources; Validation. **K.W.**: Data curation; Funding acquisition; Project administration; Resources; Supervision; Validation; Writing - review & editing.

Ethical declarations

The study protocol was approved by the ethics committees of the Affiliated Brain Hospital of Guangzhou Medical University. Written informed consent was obtained from each subject before the study.

Data availability

The datasets generated and analyzed in the current study are available from the corresponding author upon reasonable request.

Funding

This work was supported by the National Key Research and Development Program of China (2020YFC2004300, 2020YFC2004301, 2019YFC0118800, 2019YFC0118802, 2019YFC0118804, 2019YFC0118805), the National Natural Science Foundation of China (31771074, 81802230), the Guangdong Key Project in “Development of new tools for diagnosis and treatment of Autism” (2018B030335001), The scientific research project of traditional Chinese medicine of Guangdong (20211306) and the Science and Technology Program of Guangzhou (201704020168, 201704020113, 201807010064, 201803010100, 201903010032).

Acknowledgments

All procedures performed in studies involving human participants were in accordance with the ethical standards of the institutional and/or national research committee and with the 1964 Helsinki declaration and its later amendments or comparable ethical standards.

Informed consent

Informed consent was obtained from all individual participants included in the study.

References

1. Cryan, J. F. *et al.* The Microbiota-Gut-Brain Axis. *Physiological reviews* **99**, 1877-2013, doi:10.1152/physrev.00018.2018 (2019).
2. Nguyen, T. T. *et al.* Differences in gut microbiome composition between persons with chronic schizophrenia and healthy comparison subjects. *Schizophr Res* **204**, 23-29, doi:10.1016/j.schres.2018.09.014 (2019).

3. Schwarz, E. *et al.* Analysis of microbiota in first episode psychosis identifies preliminary associations with symptom severity and treatment response. *Schizophr Res* **192**, 398-403, doi:10.1016/j.schres.2017.04.017 (2018).
4. Li, S. *et al.* Altered gut microbiota associated with symptom severity in schizophrenia. *PeerJ* **8**, e9574, doi:10.7717/peerj.9574 (2020).
5. Desbonnet, L., Clarke, G., Shanahan, F., Dinan, T. G. & Cryan, J. F. Microbiota is essential for social development in the mouse. *Molecular Psychiatry* **19**, 146-148, doi:10.1038/mp.2013.65 (2014).
6. Sampson, T. R. *et al.* Gut Microbiota Regulate Motor Deficits and Neuroinflammation in a Model of Parkinson's Disease. *Cell* **167**, 1469-1480.e1412, doi:https://doi.org/10.1016/j.cell.2016.11.018 (2016).
7. Nemani, K., Hosseini Ghomi, R., McCormick, B. & Fan, X. Schizophrenia and the gut-brain axis. *Progress in neuro-psychopharmacology & biological psychiatry* **56**, 155-160, doi:10.1016/j.pnpbp.2014.08.018 (2015).
8. Cepeda, M. S., Katz, E. G. & Blacketer, C. Microbiome-Gut-Brain Axis: Probiotics and Their Association With Depression. *The Journal of neuropsychiatry and clinical neurosciences* **29**, 39-44, doi:10.1176/appi.neuropsych.15120410 (2017).
9. Hu, S. *et al.* Gut Microbiota Changes in Patients with Bipolar Depression. *Advanced Science* **6**, 1900752, doi:10.1002/advs.201900752 (2019).
10. Tomova, A. *et al.* Gastrointestinal microbiota in children with autism in Slovakia. *Physiology & Behavior* **138**, 179-187, doi:https://doi.org/10.1016/j.physbeh.2014.10.033 (2015).
11. Cattaneo, A. *et al.* Association of brain amyloidosis with pro-inflammatory gut bacterial taxa and peripheral inflammation markers in cognitively impaired elderly. *Neurobiology of Aging* **49**, 60-68, doi:https://doi.org/10.1016/j.neurobiolaging.2016.08.019 (2017).
12. Caputi, V. & Giron, M. C. Microbiome-Gut-Brain Axis and Toll-Like Receptors in Parkinson's Disease. *International journal of molecular sciences* **19**, doi:10.3390/ijms19061689 (2018).
13. Sudo, N. *et al.* Postnatal microbial colonization programs the hypothalamic-pituitary-adrenal system for stress response in mice. *The Journal of physiology* **558**, 263-275, doi:10.1113/jphysiol.2004.063388 (2004).
14. Nguyen, T. T., Kosciolek, T., Eyler, L. T., Knight, R. & Jeste, D. V. Overview and systematic review of studies of microbiome in schizophrenia and bipolar disorder. *Journal of psychiatric research* **99**, 50-61, doi:10.1016/j.jpsychires.2018.01.013 (2018).
15. Saha, S., Chant, D. & McGrath, J. A systematic review of mortality in schizophrenia: is the differential mortality gap worsening over time? *Archives of general psychiatry* **64**, 1123-1131, doi:10.1001/archpsyc.64.10.1123 (2007).
16. Guimond, S. *et al.* Functional connectivity associated with improvement in emotion management after cognitive enhancement therapy in early-course schizophrenia. *Psychological medicine*, 1-10, doi:10.1017/s0033291720004110 (2020).
17. van Erp, T. G. M. *et al.* Cortical Brain Abnormalities in 4474 Individuals With Schizophrenia and 5098 Control Subjects via the Enhancing Neuro Imaging Genetics Through Meta Analysis (ENIGMA) Consortium. *Biological psychiatry* **84**, 644-654, doi:10.1016/j.biopsych.2018.04.023 (2018).
18. Jiang, Y. *et al.* Insular changes induced by electroconvulsive therapy response to symptom improvements in schizophrenia. *Progress in neuro-psychopharmacology & biological psychiatry* **89**, 254-262, doi:10.1016/j.pnpbp.2018.09.009 (2019).

19. Brandl, F. *et al.* Specific Substantial Dysconnectivity in Schizophrenia: A Transdiagnostic Multimodal Meta-analysis of Resting-State Functional and Structural Magnetic Resonance Imaging Studies. *Biological psychiatry* **85**, 573-583, doi:10.1016/j.biopsych.2018.12.003 (2019).
20. Wang, S. *et al.* Abnormal regional homogeneity as a potential imaging biomarker for adolescent-onset schizophrenia: A resting-state fMRI study and support vector machine analysis. *Schizophrenia research* **192**, 179-184, doi:10.1016/j.schres.2017.05.038 (2018).
21. Jiang, L. & Zuo, X. N. Regional Homogeneity: A Multimodal, Multiscale Neuroimaging Marker of the Human Connectome. *The Neuroscientist : a review journal bringing neurobiology, neurology and psychiatry* **22**, 486-505, doi:10.1177/1073858415595004 (2016).
22. Ji, L. *et al.* Characterizing functional regional homogeneity (ReHo) as a B-SNIP psychosis biomarker using traditional and machine learning approaches. *Schizophrenia research* **215**, 430-438, doi:10.1016/j.schres.2019.07.015 (2020).
23. Zang, Y., Jiang, T., Lu, Y., He, Y. & Tian, L. Regional homogeneity approach to fMRI data analysis. *NeuroImage* **22**, 394-400, doi:10.1016/j.neuroimage.2003.12.030 (2004).
24. Xiao, B. *et al.* Abnormalities of localized connectivity in schizophrenia patients and their unaffected relatives: a meta-analysis of resting-state functional magnetic resonance imaging studies. *Neuropsychiatric disease and treatment* **13**, 467-475, doi:10.2147/ndt.S126678 (2017).
25. Guo, W. *et al.* Cerebellar abnormalities in first-episode, drug-naive schizophrenia at rest. *Psychiatry research. Neuroimaging* **276**, 73-79, doi:10.1016/j.pscychresns.2018.03.010 (2018).
26. Gong, J. *et al.* Abnormalities of intrinsic regional brain activity in first-episode and chronic schizophrenia: a meta-analysis of resting-state functional MRI. *Journal of psychiatry & neuroscience : JPN* **45**, 55-68, doi:10.1503/jpn.180245 (2020).
27. Shen, Y. *et al.* Analysis of gut microbiota diversity and auxiliary diagnosis as a biomarker in patients with schizophrenia: A cross-sectional study. *Schizophr Res* **197**, 470-477, doi:10.1016/j.schres.2018.01.002 (2018).
28. Cheng, S. *et al.* Identifying psychiatric disorder-associated gut microbiota using microbiota-related gene set enrichment analysis. *Briefings in bioinformatics* **21**, 1016-1022, doi:10.1093/bib/bbz034 (2020).
29. Hoyles, L. & Swann, J. in *The Handbook of Metabolic Phenotyping* (eds John C. Lindon, Jeremy K. Nicholson, & Elaine Holmes) 535-560 (Elsevier, 2019).
30. Kelly, J. R. *et al.* Transferring the blues: Depression-associated gut microbiota induces neurobehavioural changes in the rat. *Journal of psychiatric research* **82**, 109-118, doi:https://doi.org/10.1016/j.jpsychires.2016.07.019 (2016).
31. Vrieze, A. *et al.* Transfer of Intestinal Microbiota From Lean Donors Increases Insulin Sensitivity in Individuals With Metabolic Syndrome. *Gastroenterology* **143**, 913-916.e917, doi:https://doi.org/10.1053/j.gastro.2012.06.031 (2012).
32. Morris, G. *et al.* The Role of the Microbial Metabolites Including Tryptophan Catabolites and Short Chain Fatty Acids in the Pathophysiology of Immune-Inflammatory and Neuroimmune Disease. *Molecular Neurobiology* **54**, 4432-4451, doi:10.1007/s12035-016-0004-2 (2017).
33. Li, J. *et al.* Clostridiales are predominant microbes that mediate psychiatric disorders. *Journal of psychiatric research* **130**, 48-56, doi:https://doi.org/10.1016/j.jpsychires.2020.07.018 (2020).
34. Sun, T. *et al.* Distinct Associations of Cognitive Impairments and Reduced Gray Matter Volumes in Remitted Patients with Schizophrenia and Bipolar Disorder. *Neural plasticity* **2020**, 8859388,

doi:10.1155/2020/8859388 (2020).

35. Brown, G. G. *et al.* Voxel-based morphometry of patients with schizophrenia or bipolar I disorder: a matched control study. *Psychiatry research* **194**, 149-156, doi:10.1016/j.pscychresns.2011.05.005 (2011).
36. Van Rheenen, T. E. *et al.* Widespread Volumetric Reductions in Schizophrenia and Schizoaffective Patients Displaying Compromised Cognitive Abilities. *Schizophrenia bulletin* **44**, 560-574, doi:10.1093/schbul/sbx109 (2018).
37. Kanai, R. & Rees, G. The structural basis of inter-individual differences in human behaviour and cognition. *Nature reviews. Neuroscience* **12**, 231-242, doi:10.1038/nrn3000 (2011).
38. Zhao, X. *et al.* Abnormalities of regional homogeneity and its correlation with clinical symptoms in Naïve patients with first-episode schizophrenia. *Brain imaging and behavior* **13**, 503-513, doi:10.1007/s11682-018-9882-4 (2019).
39. Levitt, J. J., Bobrow, L., Lucia, D. & Srinivasan, P. A selective review of volumetric and morphometric imaging in schizophrenia. *Current topics in behavioral neurosciences* **4**, 243-281, doi:10.1007/7854_2010_53 (2010).
40. Shenton, M. E. *et al.* Abnormalities of the left temporal lobe and thought disorder in schizophrenia. A quantitative magnetic resonance imaging study. *The New England journal of medicine* **327**, 604-612, doi:10.1056/nejm199208273270905 (1992).
41. Fujiwara, H. *et al.* Female specific anterior cingulate abnormality and its association with empathic disability in schizophrenia. *Progress in neuro-psychopharmacology & biological psychiatry* **32**, 1728-1734, doi:10.1016/j.pnpbp.2008.07.013 (2008).
42. Liang, Y. *et al.* Amplitude of low-frequency fluctuations in childhood-onset schizophrenia with or without obsessive-compulsive symptoms: a resting-state functional magnetic resonance imaging study. *Archives of medical science : AMS* **15**, 126-133, doi:10.5114/aoms.2018.73422 (2019).
43. Lui, S. *et al.* Short-term effects of antipsychotic treatment on cerebral function in drug-naive first-episode schizophrenia revealed by "resting state" functional magnetic resonance imaging. *Archives of general psychiatry* **67**, 783-792, doi:10.1001/archgenpsychiatry.2010.84 (2010).
44. Xu, J., Qin, W., Liu, B., Jiang, T. & Yu, C. Interactions of genetic variants reveal inverse modulation patterns of dopamine system on brain gray matter volume and resting-state functional connectivity in healthy young adults. *Brain structure & function* **221**, 3891-3901, doi:10.1007/s00429-015-1134-4 (2016).
45. Wu, F. *et al.* Structural and functional brain abnormalities in drug-naive, first-episode, and chronic patients with schizophrenia: a multimodal MRI study. *Neuropsychiatric disease and treatment* **14**, 2889-2904, doi:10.2147/ndt.S174356 (2018).
46. Walton, E. *et al.* The impact of genome-wide supported schizophrenia risk variants in the neurogranin gene on brain structure and function. *PloS one* **8**, e76815, doi:10.1371/journal.pone.0076815 (2013).
47. Ji, Y. *et al.* Genes associated with gray matter volume alterations in schizophrenia. *NeuroImage* **225**, 117526, doi:10.1016/j.neuroimage.2020.117526 (2021).
48. Tengeler, A. C. *et al.* Gut microbiota from persons with attention-deficit/hyperactivity disorder affects the brain in mice. *Microbiome* **8**, 44, doi:10.1186/s40168-020-00816-x (2020).
49. Tillisch, K. *et al.* Brain Structure and Response to Emotional Stimuli as Related to Gut Microbial Profiles in Healthy Women. *Psychosomatic medicine* **79**, 905-913, doi:10.1097/psy.0000000000000493 (2017).
50. Janes, A. C., Farmer, S., Frederick, B., Nickerson, L. D. & Lukas, S. E. An increase in tobacco craving is associated with enhanced medial prefrontal cortex network coupling. *PloS one* **9**, e88228,

doi:10.1371/journal.pone.0088228 (2014).

51. Wu, P. C., Tu, M. S., Lin, P. H., Chen, Y. S. & Tsai, H. C. Prevotella brain abscesses and stroke following dental extraction in a young patient: a case report and review of the literature. *Internal medicine (Tokyo, Japan)* **53**, 1881-1887, doi:10.2169/internalmedicine.53.1299 (2014).
52. Lin, D. *et al.* Association between the oral microbiome and brain resting state connectivity in smokers. *NeuroImage* **200**, 121-131, doi:10.1016/j.neuroimage.2019.06.023 (2019).
53. Pizza, M. & Rappuoli, R. Neisseria meningitidis: pathogenesis and immunity. *Current opinion in microbiology* **23**, 68-72, doi:10.1016/j.mib.2014.11.006 (2015).
54. Puntis, S. *et al.* Specialised early intervention teams (extended time) for recent-onset psychosis. *The Cochrane database of systematic reviews* **11**, Cd013287, doi:10.1002/14651858.CD013287.pub2 (2020).
55. Petrolini, V., Jorba, M. & Vicente, A. The Role of Inner Speech in Executive Functioning Tasks: Schizophrenia With Auditory Verbal Hallucinations and Autistic Spectrum Conditions as Case Studies. *Frontiers in psychology* **11**, 572035, doi:10.3389/fpsyg.2020.572035 (2020).
56. Singh, K., Singh, S. & Malhotra, J. Spectral features based convolutional neural network for accurate and prompt identification of schizophrenic patients. *Proceedings of the Institution of Mechanical Engineers. Part H, Journal of engineering in medicine*, 954411920966937, doi:10.1177/0954411920966937 (2020).
57. Dhiman, R. K. Gut microbiota and hepatic encephalopathy. *Metabolic Brain Disease* **28**, 321-326, doi:10.1007/s11011-013-9388-0 (2013).
58. Gao, W. *et al.* Gut microbiome and brain functional connectivity in infants-a preliminary study focusing on the amygdala. *Psychopharmacology* **236**, 1641-1651, doi:10.1007/s00213-018-5161-8 (2019).
59. van Leeuwen, T. M. *et al.* Perceptual Gains and Losses in Synesthesia and Schizophrenia. *Schizophrenia bulletin*, doi:10.1093/schbul/sbaa162 (2020).
60. Ashburner, J. A fast diffeomorphic image registration algorithm. *NeuroImage* **38**, 95-113, doi:10.1016/j.neuroimage.2007.07.007 (2007).
61. Song, J. *et al.* Altered gray matter structural covariance networks at both acute and chronic stages of mild traumatic brain injury. *Brain imaging and behavior*, doi:10.1007/s11682-020-00378-4 (2020).
62. Dai, Z. *et al.* Discriminative analysis of early Alzheimer's disease using multi-modal imaging and multi-level characterization with multi-classifier (M3). *NeuroImage* **59**, 2187-2195, doi:10.1016/j.neuroimage.2011.10.003 (2012).
63. Chao-Gan, Y. & Yu-Feng, Z. DPARSF: A MATLAB Toolbox for "Pipeline" Data Analysis of Resting-State fMRI. *Frontiers in systems neuroscience* **4**, 13, doi:10.3389/fnsys.2010.00013 (2010).
64. Bolyen, E. *et al.* Reproducible, interactive, scalable and extensible microbiome data science using QIIME 2. *Nature Biotechnology* **37**, 852-857, doi:10.1038/s41587-019-0209-9 (2019).
65. Meyts, I. & Aksentijevich, I. Deficiency of Adenosine Deaminase 2 (DADA2): Updates on the Phenotype, Genetics, Pathogenesis, and Treatment. *Journal of clinical immunology* **38**, 569-578, doi:10.1007/s10875-018-0525-8 (2018).
66. Oksanen, J. *et al.* vegan: Community Ecology Package, v. 2.3–5. (2016).
67. Yee, T. W. & Hadi, A. F. Row–-column interaction models, with an R implementation. *Comput. Stat.* **29**, 1427–1445, doi:10.1007/s00180-014-0499-9 (2014).

Figures

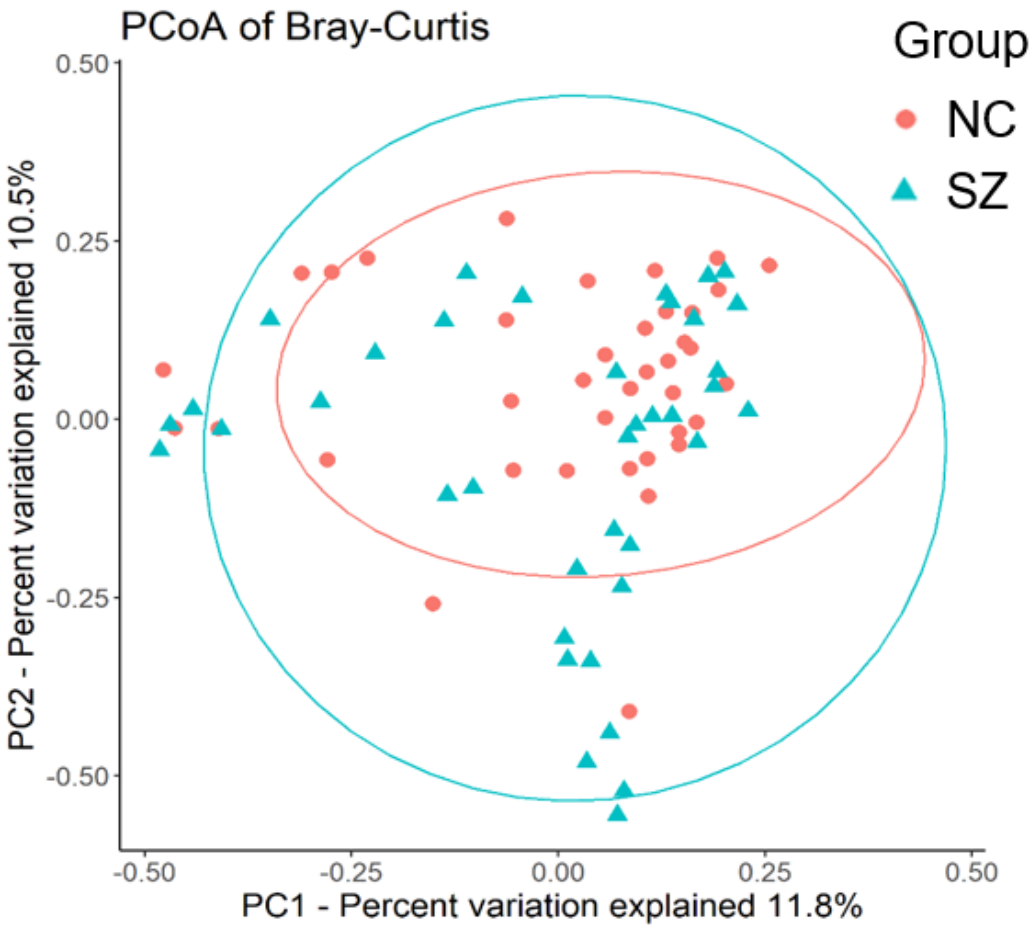

Figure 1

PCoA plot illustrating beta diversity distance matrices of Bray-Curtis distance comparing sample distribution between the two groups. The red dots represent NCs, and the green triangles represent SZs.

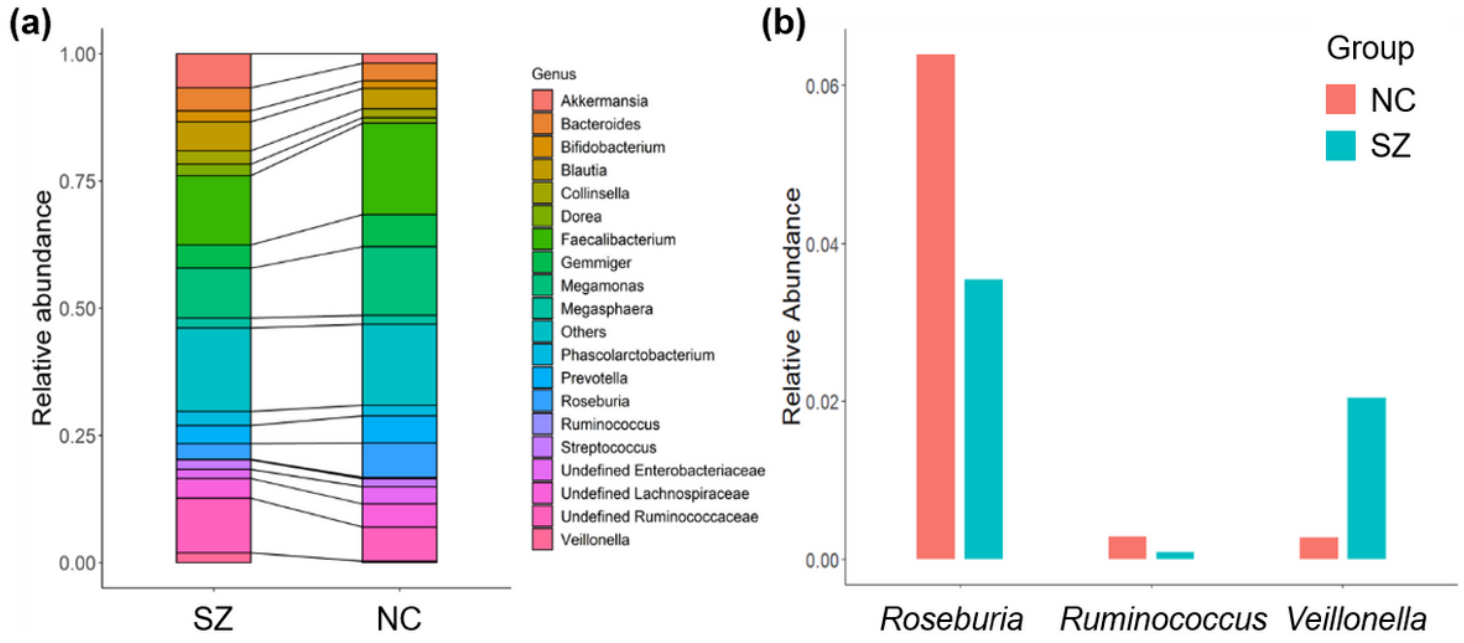

Figure 2

Microbial composition at the genus level. (a) Summary of the most abundant genera in the NC and SZ groups. (b) Bacterial genera that were significantly different between the two groups ($p < 0.05$, uncorrected).

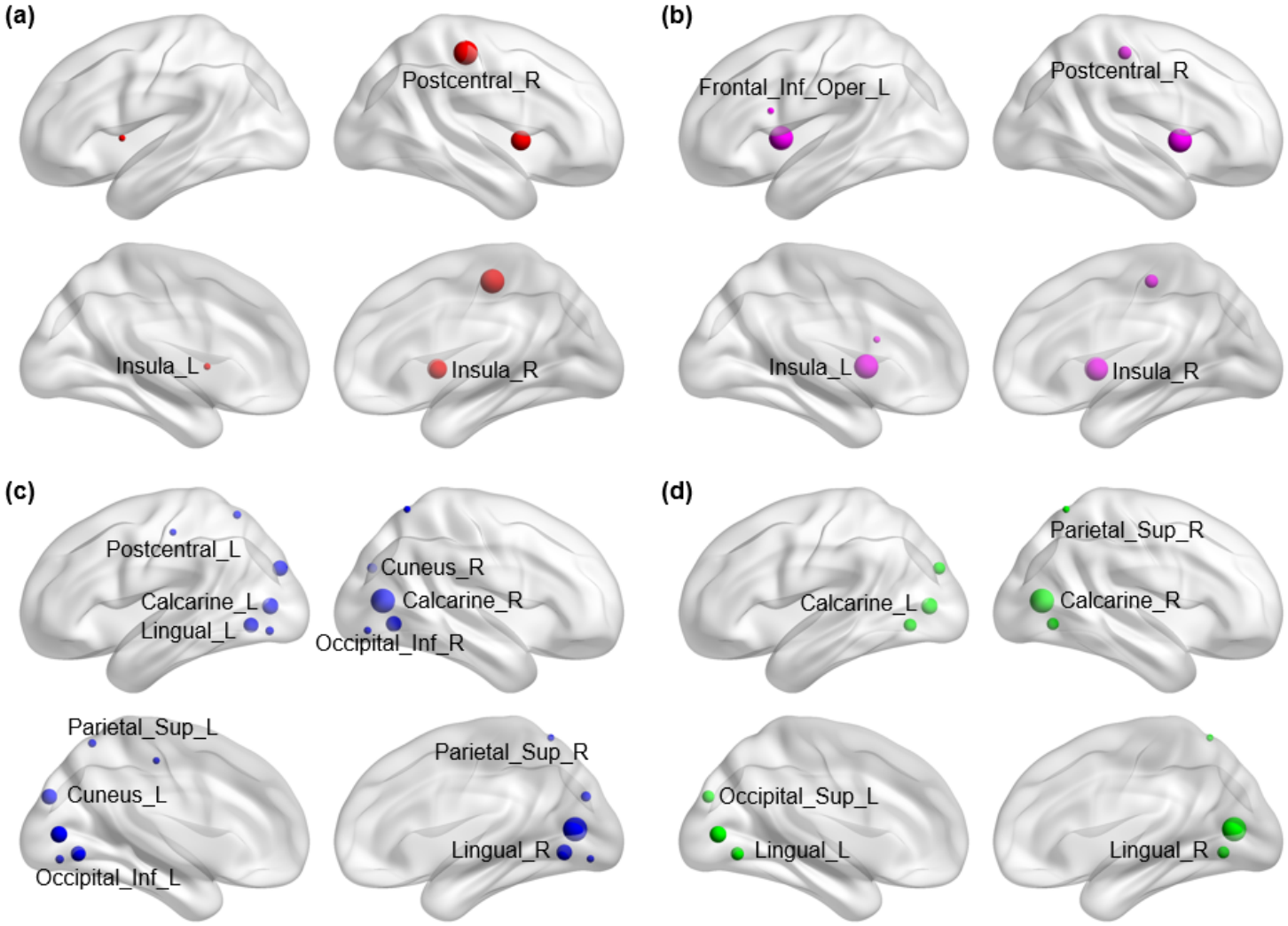

Figure 3

Brain regions segmented by the AAL atlas showing significant differences in GMV and ReHo indexes between the SZs and the NCs, and a significant correlation between the residuals of the GMV as well as ReHo indexes and the residuals of the alpha diversity in SZs. (a) Brain regions showing significant correlation between the residuals of GMV index and the observed species of alpha diversity. (b) Brain regions showing significant correlation between the residuals of GMV index and the Faith_PD of alpha diversity. (c) Brain regions showing significant correlation between the residuals of ReHo index and evenness of alpha diversity. (d) Brain regions showing significant correlation between the residuals of ReHo index and Shannon of alpha diversity. Notes: the size of the nodes means the relative size of the r values. Sup, superior; Inf, inferior; L (R), left (right) hemisphere.

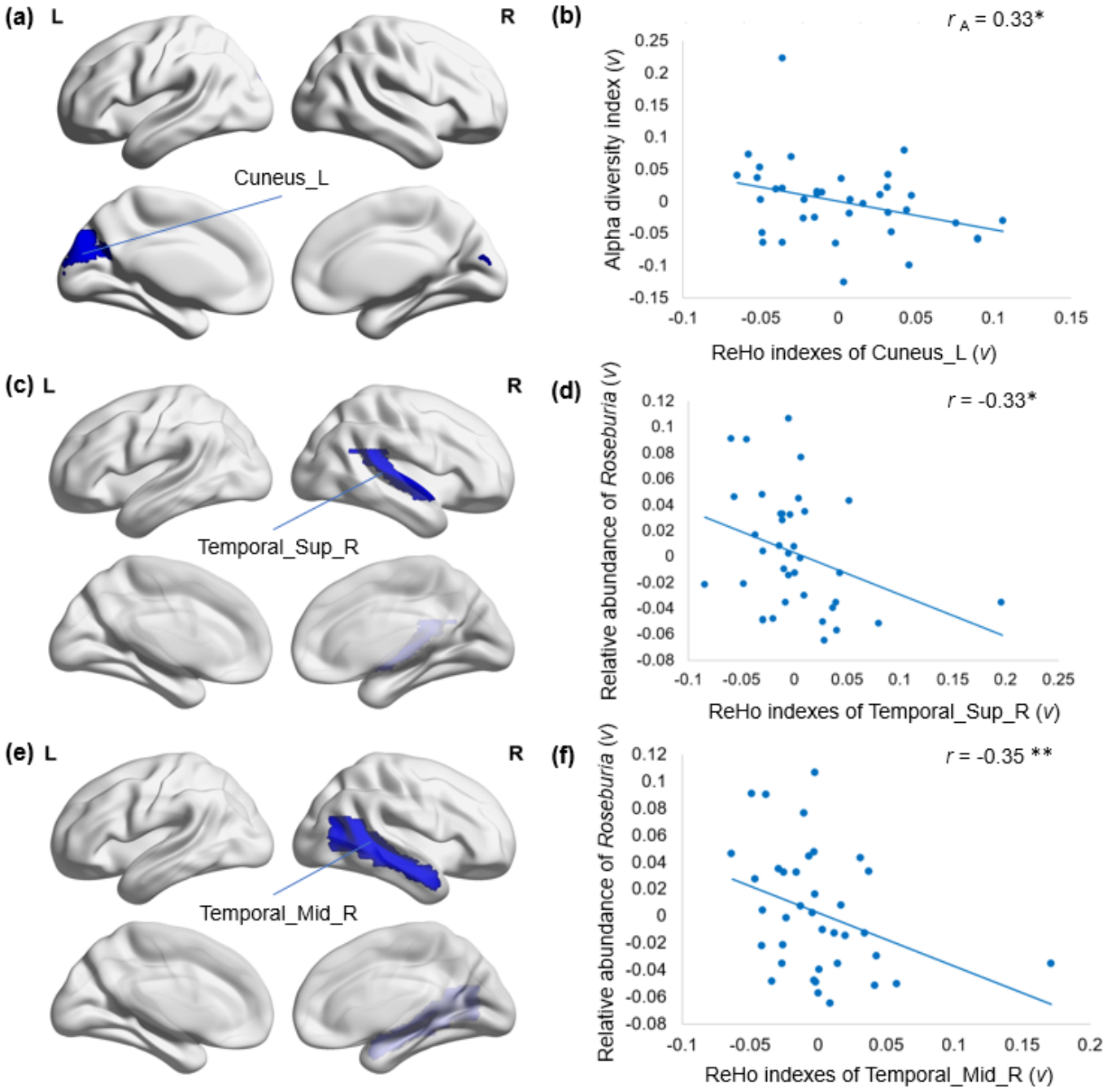

Figure 4

Brain regions segmented by the AAL atlas showing significant differences in ReHo indexes between the SZs and the NCs and a significant correlation between the residuals of the ReHo indexes and the residuals of the residuals of relative abundance of Roseburia in SZs. (a) Cuneus_L showed significantly decreased ReHo indexes in SZs compared with the NCs ($p < 0.05$). (b) The residuals of the ReHo indexes in Cuneus_L were significantly negatively correlated with the residuals of the relative abundance of Roseburia in SZs. (c) Temporal_Sup_R showed significantly decreased ReHo indexes in SZs compared with the NCs ($p < 0.05$). (d) The residuals of the ReHo indexes in Temporal_Sup_R were significantly negatively correlated with the residuals of the relative abundance of Roseburia in SZs. (e) Temporal_Mid_R showed significantly decreased ReHo indexes in the SZs compared with the NCs ($p < 0.05$). (f) The residuals of ReHo indexes in Temporal_Mid_R were significantly negatively correlated with

the residuals of the relative abundance of Roseburia in SZs. Abbreviations: Sup, superior; Mid, middle; v, the residuals; L (R), left (right) hemisphere; **p < 0.05, FDR corrected, *p = 0.05, FDR corrected.

Supplementary Files

This is a list of supplementary files associated with this preprint. Click to download.

- SupplementarymaterialsThegutmicrobiomewasassociatedwithbrainstructureandfunctioninschizophrenia.docx